



# Deformation Pattern of Metro Foundation Pits in Coastal Areas of China: A Statistical Analysis

Qing Cao<sup>1</sup>, Junjie Yuan<sup>1</sup>, Xuqun Zhang<sup>2</sup>, Pei Tai<sup>1,3\*</sup>, Rui Chen<sup>1,3</sup>

<sup>1</sup> School of Civil and Environmental Engineering, Harbin Institute of Technology, Shenzhen, Shenzhen, Guangdong, 518055, China

<sup>2</sup> Guangzhou Metro Design & Research Institute Co., Ltd, Guangzhou, Guangdong, 510010, China

<sup>3</sup> Guangdong Provincial Key Laboratory of Intelligent and Resilient Structures for Civil Engineering, Shenzhen 518055, China

\*Corresponding author's e-mail: [taipei@hit.edu.cn](mailto:taipei@hit.edu.cn)

**Abstract.** In coastal regions of China, extensive areas are characterized by deep and thick silty clay deposits, necessitating excavation and support during engineering construction. This study gathers excavation examples from existing literature and aims to summarize and analyze the deformation characteristics of support structures and the soil behind these structures (supporting walls) resulting from excavation. The findings demonstrate a general trend of increasing maximum lateral displacement of the supporting wall with greater excavation depth. The ratio of maximum lateral displacement to excavation depth falls within the range of 0.18% to 0.64%, while the insertion ratio spans from 0.78 to 1.23. The ratio of maximum ground settlement behind the wall to excavation depth varies between 0.28% and 0.82%. Additionally, the ratio of maximum ground settlement behind the wall to the maximum lateral displacement of the wall ranges from 0.93 to 1.81. The statistical analysis results presented here offer valuable references for the design and construction of excavations in regions characterized by deep and thick silty clay deposits. Moreover, the statistical results can serve as qualitative verification for finite element analysis in specific cases.

**Keywords:** Statistical analysis; Silty clay; Excavation; Support structures

## 1 INTRODUCTION

There are extensive areas with deep and thick silty clay in coastal regions of China <sup>[1, 2, 3]</sup>, posing frequent challenges related to excavation and support in engineering construction <sup>[4, 5]</sup>. The deformation characteristics exhibited during the excavation process of foundation pits are always assessed through finite element numerical analysis <sup>[6]</sup>. The finite element numerical analysis method can reflect the influence of various key factors on the excavation of foundation pits. Additionally, it can dynamically simulate the excavation process, allowing for a more in-depth analysis of the mechanisms and

characteristics of pit deformation [7]. However, on one hand, due to the complexity of practical engineering, finite element numerical analysis is still unable to fully consider all the various factors encountered in actual projects [8]. On the other hand, the existing constitutive models have limitations in representing various soil mechanical properties, resulting in insufficient accuracy in finite element results [9]. For example, compared to the deformation of retaining structures, there are accuracy deficiencies in the finite element method regarding the deformation characteristics of the ground behind the wall [10]. Alternatively, statistical analysis of engineering field measurements can also be helpful as an empirical reference [11, 12]. This study collects reported excavation examples of foundation pits in sites with deep and thick silty clay layers from literature, summarizes and analyses the deformation characteristics caused by excavation. Then, statistical methods are adopted to analyse the deformation characteristics exhibited during the excavation of foundation pits in such sites. The deformation patterns revealed through statistical analysis of engineering examples can not only help gain more understanding of foundation pits in such type of sites, but also serve as references for engineers in the design and construction of similar foundation pits in sites with deep and thick silty clay layers. The summarized empirical patterns also provide a useful estimation for the finite element numerical analysis, to verify its practicality and reliability in terms of deformation prediction.

## 2 DATA SOURCES

To better understand the excavation-induced deformations obtained in field measurements, the following explanations are provided for frequently used deformation parameters of the excavation pit, as shown in Figure 1.

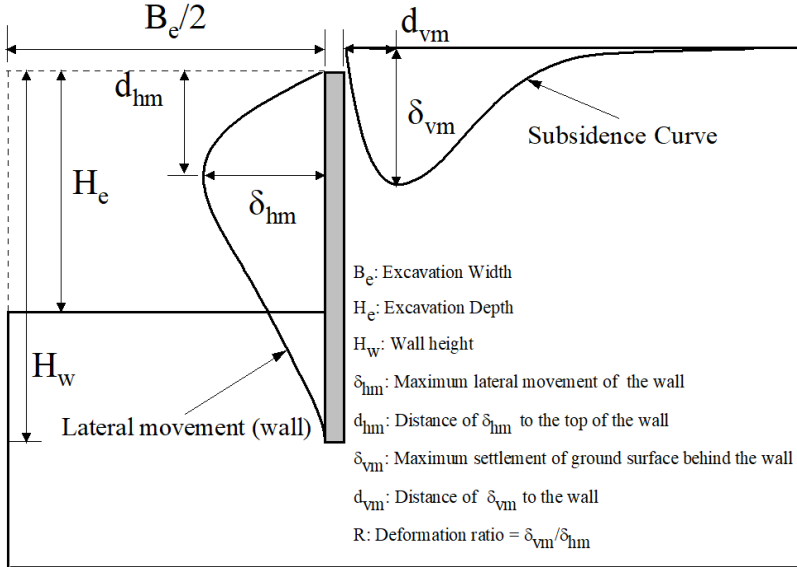


Fig. 1. Schematic diagram of various deformations related to foundation pit excavation.

As shown in Figure 1,  $B_e$  is the excavation width,  $H_e$  is the excavation depth,  $H_w$  is the depth of the supporting wall,  $\delta_{hm}$  is the maximum lateral movement of the wall,  $\delta_{vm}$  is the maximum settlement of the ground surface behind the wall,  $d_{vm}$  is the maximum settlement position of the ground surface behind the wall, and  $R$  is the deformation ratio, which is defined as  $\delta_{vm}/\delta_{hm}$ .

To analyze the deformation characteristics of deep silty soil excavation sites, 13 projects were collected from the coast area of China, including Shanghai, Ningbo and Guangzhou city, as shown in Table 1. In Shanghai and Ningbo region, the soft soil layers mainly refer to silty clay and muddy clay, which usually has a thickness greater than 10 meters and 25 meters, respectively. In Guangzhou area, the soft soil is mainly marine clay and muddy clay, which is about 10-meter-thick. All cases employed underground continuous wall support as the retaining structure.

**Table 1.** Deformation data of foundation pit in deep silt field.

Number	Project Name	$H_e/m$	$H_w/m$	$h/m$	$\delta_{hm}/mm$	$\delta_{vm}/mm$	$R$
1	R1 Line South Shaanxi Road Station <sup>[13]</sup>	14.2	30	—	64.5	76.7	1.19
2	R1 Line Sangjikan Station <sup>[13]</sup>	14	26	3.23	50	46.5	0.93
3	Line M8 Huangxing Road Station <sup>[13]</sup>	14.7	26.5	3.50	39.2	70	1.79
4	Line 2 Henanzhong Road Station <sup>[13]</sup>	15.2	30.4	2.53	97.8	101	1.03
5	R1 Line People's Square Station <sup>[13]</sup>	13.5	24.4	—	72.5	110	1.52
6	Yanchang Road Station <sup>[13]</sup>	15.2	27	3.30	62.6	74.3	1.19
7	Drumtower Station <sup>[14]</sup>	23.8	48	2.44	106.0	123.8	1.17
8	Dongmen Station <sup>[14]</sup>	22.4	40	2.47	69.7	121.4	1.74
9	Jiangxia Qiaodong Station <sup>[14]</sup>	16.8	32	2.67	41.0	63.7	1.55
10	Fu Ming Road Station (Phase II) <sup>[14]</sup>	16.3	36.3	2.44	64.6	89.3	1.38
11	Ximenkou Station <sup>[14]</sup>	16.1	33.8	2.48	28.7	45.0	1.57
12	Zeomin Station <sup>[14]</sup>	15.9	30.5	2.46	57.0	103.3	1.81
13	Cisha Station	13.2	27.3	2	26.34	36.77	1.40

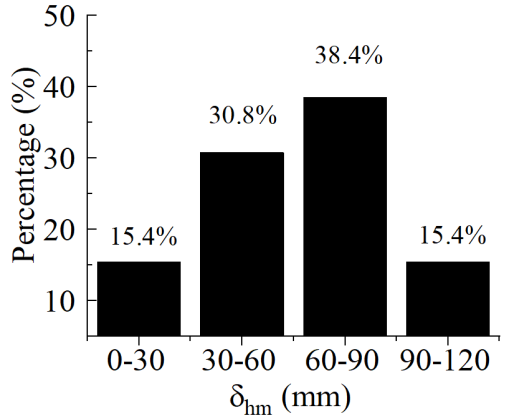
Note:  $h$  is the average vertical spacing of the supports.

### 3 DEFORMATION OF SUPPORTING STRUCTURE

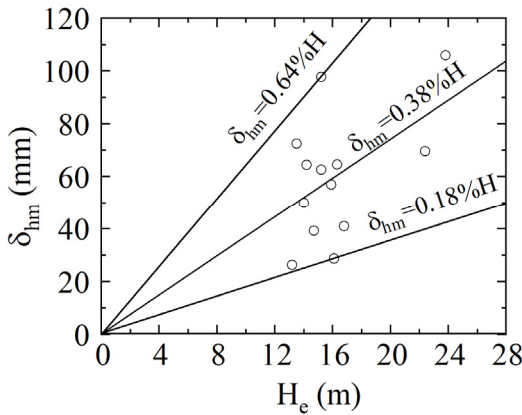
The deformation of retaining structures includes horizontal deformation (lateral displacement) and vertical deformation (settlement). The analysis of vertical deformation primarily concentrates on the vertical displacement of the top of the wall. In the excavation process of foundation pits, the uplift of the soil inside the pit induces a certain degree of upward movement of the wall. Additionally, factors such as the weight of supports or floor slabs, as well as the removal of sediment at the bottom of the wall, also influence the vertical displacement to some extent. Therefore, the wall may experience upward or downward movement.

Hereby focus are mainly on the analysis of the horizontal deformation of a common retaining structure in subway foundation pits, namely, underground diaphragm walls. Horizontal deformation encompasses three key aspects: the mode of horizontal deformation, the magnitude of maximum horizontal displacement, and its corresponding location. The horizontal deformation of the wall is influenced by various factors in civil engineering, including the unbalanced soil pressure caused by excavation, the overall stiffness of the support system, excavation stability, and site soil conditions. The unbalanced soil pressure is further affected by factors such as excavation depth, excavation width, stability safety factor, stiffness of retaining structures, stiffness of support, spacing between supports, and pre-stress of the support. Statistical analysis of field monitoring data can be adopted to comprehensively reflect the influence of these factors on the maximum lateral displacement of the wall, as a result, the empirical relationship between excavation depth, support system stiffness, the resistance to bottom heave and the maximum lateral displacement of the wall can be drawn for engineering practice. Depending on soil conditions, types of retaining structures, support forms, and construction techniques, the magnitude of the horizontal displacement of a diaphragm wall directly affects the displacement of the surrounding soil mass, which furtherly impacts the safety of structures, pipelines, and facilities outside the excavation area.

The location of the maximum lateral displacement of the wall is primarily influenced by geological conditions, particularly the soil stratification. For instance, engineering experience in Shanghai indicates that the maximum horizontal displacement generally occurs at a certain level above the bottom of the excavation. This is because the most significant displacement occurs when excavating to the soft muddy clay soil which is with depth around 16 meters. As the excavation depth increases, the soil at the bottom is transitioning to a stiff clay layer, meanwhile, the maximum horizontal displacement does not shift downward accordingly, it would remain at the upper level of the muddy clay layer, rather than occurring at the excavation surface.



(a)



(b)

**Fig. 2.** Statistical relation of maximum lateral displacement of wall: (a) Statistical distribution of the maximum lateral displacement of the wall (b) The relationship between the maximum lateral displacement of the wall and the excavation depth.

Figure 2(a) shows the statistical distribution of the maximum lateral displacement of the diaphragm wall according to cases in Table 1. It can be observed that nearly 70% of the maximum lateral displacement of the excavation walls falls between 30 and 90 mm for excavations in sites with deep and thick soft clay layers. Among these, excavations with lateral displacements ranging from 30 to 60 mm account for 30.8% of the total, while excavations with displacements ranging from 60 to 90 mm account for 38.4%. Excavations with maximum lateral displacements between 0-30 mm and 90-120 mm both account for only 15.4%.

Additionally, Figure 2(b) illustrates the relationship between the maximum lateral displacement of diaphragm wall and the excavation depth. It is apparent that the maximum lateral displacement tends to increase with the excavation depth. The maximum lateral displacement falls in the range between 0.18% to 0.64% of the excavation

depth, with an average value of  $0.38\%H_e$ . This result was further compared to other wall deformation database in typical soft soil and hard soil regions in China, as summarized in Table 2. The comparison suggests that the statistical results of this paper are closer to the results in the similar soft soil areas [15, 18, 19], but much larger than those in stiff soils [20, 21], which indicates that stratum conditions are key factor affecting wall deformation.

**Table 2.** Deformation data of foundation pit in deep silt field.

Area	Database Description	Geologic description	Main findings
Shanghai (2008) [15]	93 cases with diaphragm walls, 52 concrete-supported, 40 steel-supported, 1 lattice diaphragm wall; Top-down method; Excavation depth 10-20 meters (up to 30.4 meter); Insertion ratio between 0.45 and 1.52, with an average of 0.88.	Silty clay and muddy clay; Burial depth 4-20 meters; Thickness 10-20 meters.	$\delta_{hmax}/H_e$ (%) ranges from 0.1 to 1.0, with a mean value of about 0.42; $\delta_{hmax}$ increases with excavation depth, occurs roughly near the excavation surface (5m above or below); $\delta_{hmax}$ and its location are almost independent of support type.
Shanghai, Hangzhou (2007) [16]	46 building foundation pits using top-down method; Supported by grouted piles and diaphragm walls; Excavation depth up to 30 m.	Muddy clay burial depth 0-2 meters, thickness 3-6 meters; Silty clay with thickness of 8-10 meters.	$\delta_{hmax}/H_e$ (%) ranges from 0.065 to 1, with an average value of 0.5; Located near the excavation surface; $\delta_{hmax}$ gradually transits from below the excavation surface to above the surface as excavation depth increases.
Taipei (1993) [17]	Supported by diaphragm wall	—	$\delta_{hmax}/H_e$ (%) is between 0.2 and 0.5; A large value for site contains a weak soil layer, a lower value for sandy soil, and a middle value for a mixed stratum.
Shanghai (2008) [18]	50 cases, supported by diaphragm walls, including metro pits and building pits; Excavation depths ranging from 8.7 to 30.4 meters.	Silty clay and muddy clay; Burial depth 4-20 meters; Thickness 10-20 meters.	$\delta_{hmax}/H_e$ (%) He<15m: 0.11~0.49, with an average of 0.26; He>15m: 0.21~0.74, with an average of 0.49.
Ningbo (2011) [19]	14 metro pits, 13 diaphragm walls, 1 SMW method; Initial concrete support and steel support;	Soft soil with thickness more than 25 meters.	$\delta_{hmax}/H_e$ (%) ranges from 0.18 to 0.93, with a mean value of 0.43; The ratio of $\delta_{hmax}$ depth to excavation depth

	Excavation depths of 16.5 meters; An average insertion ratio of 0.98.		ranges from 0.8 to 1.25, with a mean value of 0.95.
Beijing (2012) <sup>[20]</sup>	37 cases with open excavation, 10 soil nail walls (excavation depths 9.6-22.38 meters), 27 grouted piles (excavation depths 14.42-29 meters).	Hard silt and sand layers.	$\delta_{hmax}/H_e$ (%) ranges from 0.04 to 0.218, with a mean value of 0.103.
Dalian (2012) <sup>[21]</sup>	Metro pits with open excavation, with cantilevered support and inner support; Excavation depth ranges from 8.31 to 20.66 meters.	—	$\delta_{hmax}/H_e$ (%) ranges from 0.11 to 0.27, with a mean value of 0.159.
This study	Metro pits with open excavation; Excavation depth ranges from 13.5 to 23.8 meters.	Soft soil with thicknesses beyond 10 meters.	$\delta_{hmax}/H_e$ (%) ranged from 0.18 to 0.64, with a mean value of 0.38.

In addition, statistical results suggest that, as the depth increases, the maximum lateral displacement shifts from below the bottom of pit to above the excavation surface. This is mainly due to the shallow burial depth of soft soil in the coastal regions. In shallow excavations, the bottom of the pit is located within the silt layer, while it reaches a better-quality soil layer in deep excavations. This again indicates that the burial depth of soft soil has a significant influence on the maximum lateral displacement of retaining structures. Furthermore, the statistical results also show that the maximum lateral displacements in several cases exceed the control values in current standards, which is roughly 60-90 mm. However, the actual excavations remain in a safe and stable state, suggesting that the current standard are conservative to some extent. With the development of construction technique, more comprehensive control standards for excavation deformations are expected to be optimized based on an increasing database of field monitoring.

#### 4 DEFORMATION OF GROUND SURFACE BEHIND THE WALL

Soil deformation behind diaphragm walls includes horizontal displacement and vertical displacement (settlement) of the ground surface and along the depth. Currently, the vertical displacement of the ground surface, namely, ground settlement, including settlement patterns, maximum settlement, and its locations are always monitored in practice. On the other hand, the horizontal displacement at the ground surface and the deformation of the deep soil are not the primary concern.

The maximum settlement of ground surface behind the diaphragm wall is a crucial indicator which can be used in the assessment of the safety of surrounding structures, pipelines, and other infrastructure. The maximum surface settlement outside the exca-

vation pit is also closely related to factors such as soil conditions, types of retaining structures, and support forms. It can be seen that factors influencing the lateral displacement of the wall also affect the deformation of the surrounding soil. Additionally, previous experience suggests that there may exist relationships among the maximum settlement, the depth of excavation, and the maximum horizontal displacement of the retaining structure. For example, the distance of the maximum settlement point against the wall is approximately proportional to the final excavation depth. For a triangular settlement pattern, the maximum ground settlement occurs at the edge of the wall. For a groove-shaped settlement pattern, the horizontal distance from the maximum ground settlement point to the wall is generally about 0.4 to 0.7 times the final excavation depth.

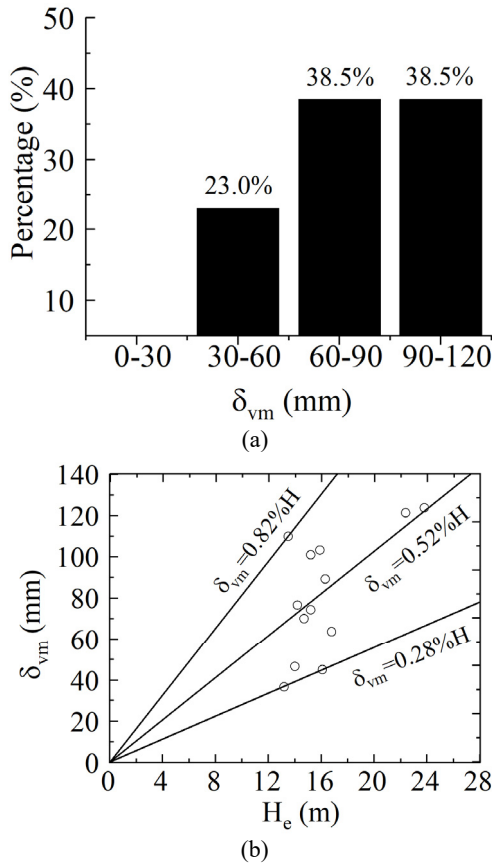


**Fig. 3.** Statistical relationship of maximum surface settlement: (a) Statistical distribution of maximum surface settlement (b) Relationship between maximum surface settlement and depth of excavation.

According to cases in Table 1, it can be observed that 77% of the maximum surface settlement values behind the wall ranges from 60 to 120 mm for excavation in soft soil sites (Figure 3a). Specifically, 38.5% of the maximum settlement is between



60 and 90 mm, while another 38.5% have a maximum settlement between 90 and 120 mm. Only 23.0% of the foundation pits have a maximum settlement between 30 and 60 mm, but there is no case with maximum surface settlement below 30 mm. Figure 3(b) further illustrates that the maximum surface settlement behind the wall increases gradually with the excavation depth, and it falls in the range of 0.28% to 0.82% of the excavation depth, with an average value of 0.52%  $H_e$ .

Similarly, the statistical result of this study was compared to the cases data in typical soft soil and hard soil regions in the literature, as summarized in Table 3.

**Table 3.** Summary of measured surface settlement statistics behind the wall in different areas.

Area	Database Description	Geologic description	Main findings
Shanghai (2011) [13]	35 cases with top-down method; 26 supported by diaphragm walls, 7 by grouted piles, and 2 by SMW method; Excavation depth ranges from 7 to 34 meters.	Silty clay and muddy clay; Burial depth 0-10.08 meters; Thickness 8.3-16.3 meters.	$\delta_{vmax}/H_e$ (%) ranges from 0.1 to 0.8, with an average of 0.38; $\delta_{vmax}$ increases with excavation depth and soft soil thickness, other factors have no significant impact. R ranges from 0.4 to 2.0, with an average of 0.84; For groove-shaped settlement, the ratio of surface settlement near the wall to excavation depth is between 0% and 0.5%, the ratio of maximum surface settlement behind the wall to excavation depth is between 0.3 and 1.0; Settlement gradually disappears within the range of 1.0-4.0 times excavation depth.
Shanghai (2008) [18]	93 cases with diaphragm walls, 52 concrete-supported, 40 steel-supported, 1 lattice diaphragm wall; Top-down method; Excavation depth 10-20 meters (up to 30.4 meter); Insertion ratio between 0.45 and 1.52, with an average of 0.88.	Silty clay and muddy clay; Burial depth 4-20 meters; Thickness 10-20 meters.	$H_e < 15m$ : $\delta_{vmax}/H_e$ (%) ranges from 0.18 to 0.48, with an average value of 0.26; R ranged from 0.43 to 1.79, with an average value of 0.92; $H_e > 15m$ : $\delta_{vmax}/H_e$ (%) ranges from 0.24 to 0.88, with an average value of 0.48; R ranged from 0.71 to 1.69, with an average value of 1.17.
Ningbo (2011) [19]	14 metro pits, 13 diaphragm walls, 1 SMW method; Initial concrete support and steel support;	Soft soil with thickness more than 25 meters.	$\delta_{vmax}/H_e$ (%) ranges from 0.15 to 1.2, with an average value of 0.69.

	Excavation depths of 16.5 meters; An average insertion ratio of 0.98.		
Beijing (2012) [22]	30 cases, top-down open excavation, supported by grouted piles, steel supports, soil nails, and pre-stressed anchor cables; Pit width around 20 meters, excavation depth mainly between 15 to 20 meters, up to 25 meters; Insertion ratio ranges from 0.3 to 0.44, with an average value of 0.36.	Quaternary alluvial deposits, silty sand, clay interbedded with sand and gravel; Hard soil area.	$\delta_{vmax}/H_e$ (%) ranges from 0.034 to 0.316, with an average value of 0.1; 75% of the surface settlement between 0 to 20 mm, 1.93% over 30 mm, 11.62% heave, decrease with excavation depth; Groove-shape settlement, maximum surface settlement point is 10 to 15 meters away from the wall, almost no deformation 30 meters away from the wall.
Dalian (2012) [21]	Metro pits with open excavation, with cantilevered support and inner support; Excavation depth ranges from 8.31 to 20.66 meters.	—	$\delta_{vmax}/H_e$ (%) ranges from 0.09 to 0.25, with an average value of 0.154.
This study	Metro pits with open excavation; Excavation depth ranges from 13.5 to 23.8 meters.	Soft soil with thicknesses beyond 10 meters.	$\delta_{vmax}/H_e$ (%) ranges from 0.28 to 0.82, with an average value of 0.52.

Based on the above comparison, it is found that the maximum ground settlement behind the wall in this study are similar to those reported in similar soft soil areas<sup>[13, 18, 19]</sup>, but significantly higher than those in commonly-seen hard soil areas<sup>[21, 22]</sup>. This finding echoes with that of maximum lateral movement, again indicating the important role of stratum conditions.

Furthermore, a close correlation between the maximum ground surface settlement behind the wall and the maximum lateral displacement of the wall can be drawn, as confirmed by numerous field measurements. This statistical relationship provides an approximate estimation for the settlement behind the wall, as illustrated in Figure 4.

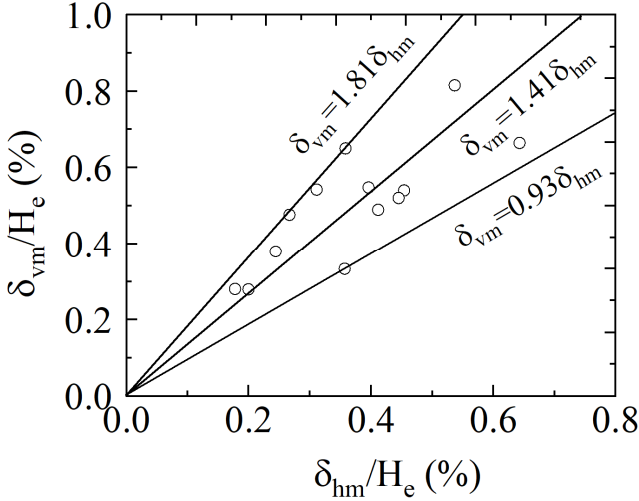


**Fig. 4.** Relationship between normalized maximum surface settlement and maximum lateral movement of the wall.

It is shown in Figure 4 that for excavation in deep and thick silty soil sites, the ratio of the maximum normalized settlement to the normalized maximum lateral wall displacement ranges from 0.93 to 1.81, with an average value of 1.41. Similar empirical relationship has also been reported based on data of foreign projects from San Francisco, Oslo, Chicago, and Taipei, where the maximum surface settlement is approximately 0.5 to 0.75 times the maximum lateral wall displacement<sup>[17]</sup>. It is recommended that the lower limit value is for excavations in sandy soil, the upper limit value is for clayey soil, and an intermediate value is for mixture of sand and clay. Specifically for weak soils, the maximum surface settlement can reach up to the same level as the maximum lateral wall displacement, which is close to the lower limit in this study. Moreover, another statistical result collected worldwide show a similar range of this ratio (0.5 to 2.0) as the current results<sup>[23, 24]</sup>. Overall, these mutual verifications provide additional confidence for the application of the proposed statistical relationship in this study.

## 5 CONCLUSIONS

13 cases of subway excavation projects in coastal areas of China with deep layers of soft clay have been collected and presented in this study, where underground diaphragm walls were used as (part of) supporting system. The lateral displacement of the wall and the ground surface settlement behind the wall were statistically analysed, and the general deformation patterns induced by excavation in sites with thick soft soil layer are summarized.

It is indicated that the maximum lateral displacement and surface settlement generally increases with the excavation depth. Some useful empirical relationships have

also been revealed statistically, which can be used for the preliminary estimation for future projects in the similar site condition. The ratio of the maximum lateral displacement to the excavation depth ranges from 0.18% to 0.64%, with an average value of 0.38%. The ratio of the maximum ground surface settlement to the excavation depth varies between 0.28% and 0.82%, with an average value of 0.52%. The ratio of the maximum ground surface settlement to the maximum lateral displacement of the wall ranges from 0.93 to 1.81, with an average value of 1.41.

This study provides a statistical database for the future excavation project in southern China, which would be useful for the deformation prediction before any sophisticated modelling being carried out. The results presented in this study could be further refined with more monitoring data available.

## ACKNOWLEDGMENTS

All authors would like to express their sincere gratitude to the National Natural Science Foundation of China (52108311), and the Shenzhen Science and Technology Program (KQTD20210811090112003 and GXWD20231130125225001) for financial supports.

## REFERENCES

1. Wang, W. (2024) Analytical methods and controlling techniques for deformation and environmental influence of deep excavations in soft soils. *Chin. J. Geotech. Eng.*, 46(01): 1-25. <https://doi.org/10.11779/CJGE20231146>.
2. Yue, X., Xie, Y., Zhang, H., Niu, Y., Zhang, S., Li, J. (2020) Study on geotechnical characteristics of marine soil at Hong Kong–Zhuhai–Macao tunnel. *Mar. Geores. Geotechnol.*, 38(6): 647-658. <https://doi.org/10.1080/1064119X.2019.1609632>.
3. Tan, Y., Lu, Y., Wang, D. (2023) Interactive behaviors of four closely spaced mega excavations in soft clays: Case study on an excavation group in Shanghai, China. *Tunn. Undergr. Space Technol.*, 138: 105186. <https://doi.org/10.1016/J.TUST.2023.105186>.
4. Sun, Y., Xiao, H. (2021) Wall displacement and ground-surface settlement caused by pit-in-pit foundation pit in soft clays. *KSCE J. Civ. Eng.*, 25(4): 1262-1275. <https://doi.org/10.1007/s12205-021-1120-8>.
5. Maher, T., Basha, A. M., Abo-Raya, M. M., Zakaria, M. H. (2022) General deformation behavior of deep excavation support systems: A review. *Global Journal of Engineering and Technology Advances*, 10(01): 039-057. <https://doi.org/10.30574/gjeta.2022.10.1.0181>.
6. Cui, J., Yang, Z., Azzam, R. (2023) Field measurement and numerical study on the effects of under-excavation and over-excavation on ultra-deep foundation pit in coastal area. *J. Mar. Sci. Eng.*, 11(1): 219. <https://doi.org/10.3390/jmse11010219>.
7. Wang, J., Xiang, H., Yan, J. (2019) Numerical simulation of steel sheet pile support structures in foundation pit excavation. *Int. J. Geomech.*, 19(4): 05019002. [https://doi.org/10.1061/\(ASCE\)GM.1943-5622.0001373](https://doi.org/10.1061/(ASCE)GM.1943-5622.0001373).
8. Wu, B., Peng, Y., Meng, G., et al. (2019) Empirical Method and Finite Element Analysis of Deep Foundation Pit Excavation in Ningbo Soft Soil. In: *IOP Conference Series: Earth and Environmental Science*. pp. 032060. <https://doi.org/10.1088/1755-1315/267/3/032060>.

9. Guan, Q. Z., Yang, Z. X., Guo, N., Hu, Z. (2023) Finite element geotechnical analysis incorporating deep learning-based soil model. *Comput. Geotech.*, 154: 105120. <https://doi.org/10.1016/j.compgeo.2022.105120>.
10. Wang, S., Li, Q., Dong, J., Wang, J., Wang, M. (2021) Comparative investigation on deformation monitoring and numerical simulation of the deepest excavation in Beijing. *Bull. Eng. Geol. Environ.*, 80: 1233-1247. <https://doi.org/10.1007/s10064-020-02019-y>.
11. Mei, Y., Li, Y. L., Wang, X. Y., et al. (2019) Statistical analysis of deformation laws of deep foundation pits in collapsible loess. *Arab. J. Sci. Eng.*, 44: 8347-8360. <https://doi.org/10.1007/s13369-019-03931-6>.
12. Xu, W., Zhang, D., Zhang, Q. (2022) Deformation behaviors and control indexes of metro-station deep excavations based on case histories. *Tunn. Undergr. Space Technol.*, 122: 104400. <https://doi.org/10.1016/j.tust.2022.104400>.
13. Wang, W., Xu, Z., Wang, J. (2011) Statistical analysis of characteristics of ground surface settlement caused by deep excavations in Shanghai soft soils. *Chin. J. Geotech. Eng.*, 33(11): 1659-1666. <https://doi.org/10.1007/s13369-019-03931-6>.
14. Zhu, Y.H., Ye, J.N., Liu, X.H. (2012) Deformation characteristics and control of foundation pits supporting with diaphragm wall in the Ningbo urban rail transit. *Hydrogeology & Engineering Geology*, 39(4): 66-74. <https://doi.org/10.1007/s10064-021-02264-9>.
15. Xu, Z., Wang J., Wang, W. (2008) Deformation Behavior of Underground Diaphragm Wall in Deep Foundation Pit Engineering in Shanghai Area. *Chinese Journal of Civil Engineering*, 2008, 41(8): 81-86.
16. Li, L., Yang, M., Xiong, J. H. (2007) Analysis of the deformation characteristics of deep excavations in soft clay. *China Civil Engineering Journal*, 40(4): 66-72. <https://doi.org/10.15951/j.tmgcxb.2007.04.012>.
17. Ou, C.Y., Hsieh, P.G., Chiou, D.C. (1993) Characteristics of Ground Surface Settlement during Excavation. *Can. Geotech. J.*, 1993(30): 758-767. <https://doi.org/10.1139/t93-068>.
18. Lu, J., Yang, M. (2008) Deformation characteristics of diaphragm walls and backfill soil in deep foundation pits in Shanghai. *Chin. J. Geotech. Eng.*, 30(Suppl.): 369-373.
19. Zheng, R., Cao, X., Liu, G., et al. (2011) Research progress on deep excavation deformation control and its practice in Ningbo area. In: *Proceedings of the 20th National Conference on Structural Engineering* .pp. 128-145. Beijing: Journal of Engineering Mechanics.
20. Li, S., Zhang, D., Fang, Q., et al. (2012) Study on deformation characteristics of deep foundation pit walls in Beijing area. *Chin. J. Rock Mech. Eng.*, 31(11): 2344-2353.
21. Ma, F.H., Hu, G.D., Yang, Q.Y., et al. (2012) Analysis of deformation characteristics of station foundation pits in Dalian area. *Journal of Liaoning Technical University (Natural Science Edition)*, 31(2): 155-158. <https://doi.org/10.3969/j.issn.1008-0562.2012.02.003>.
22. Li, S., Zhang, D. L., Fang, Q., Lu, W. (2012) Research on characteristics of ground surface deformation during deep excavation in Beijing subway. *Chin. J. Rock Mech. Eng.*, 31(1), 189-198. <https://doi.org/10.3969/j.issn.1000-6915.2012.01.022>.
23. Moormann, C. (2004) Analysis of wall and ground movements due to deep excavations in soft soil based on a new worldwide database. *Soils Found.*, 44(1), 87-98. <https://doi.org/10.3208/sandf.44.87>.
24. Tan, Y., Fan, D., & Lu, Y. (2022) Statistical analyses on a database of deep excavations in Shanghai soft clays in China from 1995–2018. *Pract. Period. Struct. Des. Constr.*, 27(1), 04021067. [https://doi.org/10.1061/\(ASCE\)SC.1943-5576.0000646](https://doi.org/10.1061/(ASCE)SC.1943-5576.0000646).

**Open Access** This chapter is licensed under the terms of the Creative Commons Attribution-NonCommercial 4.0 International License (<http://creativecommons.org/licenses/by-nc/4.0/>), which permits any noncommercial use, sharing, adaptation, distribution and reproduction in any medium or format, as long as you give appropriate credit to the original author(s) and the source, provide a link to the Creative Commons license and indicate if changes were made.

The images or other third party material in this chapter are included in the chapter's Creative Commons license, unless indicated otherwise in a credit line to the material. If material is not included in the chapter's Creative Commons license and your intended use is not permitted by statutory regulation or exceeds the permitted use, you will need to obtain permission directly from the copyright holder.

